Phonon anomaly at the charge ordering transition in $1T$-TaS_2

L. V. Gasparov and K. G. Brown
University of North Florida, Department of Chemistry and Physics, 4567 St. Johns Bluff Road, South Jacksonville, Florida 32224

A. C. Wint and D. B. Tanner
University of Florida, Department of Physics, P.O. Box 118440, Gainesville, Florida 32611-8440

H. Berger, G. Margaritondo, R. Gaál, and L. Forró
Institute of Physics of Complex Matter, Ecole Polytechnique Fédéral de Lausanne, CH-1015 Lausanne, Switzerland
(Received 13 May 2002; revised manuscript received 17 July 2002; published 10 September 2002)

The infrared reflectance of the transition-metal chalcogenide $1T$-TaS_2 has been measured at temperatures from 30 K to 360 K over 30–45 000 cm^{-1} (4 meV–5.5 eV). The optical conductivity was obtained by Kramers-Kronig analysis. At 360 K only modest traces of the phonon lines are noticeable. The phonon modes are followed by a pseudo-gap-like increase of the optical conductivity, with direct optical transitions observed at frequencies above 1 eV. As the temperature decreases, the low-frequency conductivity also decreases, phonon modes become more pronounced, and a pseudogap develops into a gap at 800 cm^{-1} (100 meV). We observe an anomalous frequency dependence of the 208 cm^{-1} infrared-active phonon mode. This mode demonstrates softening as the temperature decreases below the 180-K transition. The same mode demonstrates strong hysteresis of the frequency and linewidth changes, similar in its temperature behavior to the hysteresis in the dc resistivity. We discuss a possible relation of the observed softening of the mode to the structural changes and changes in electronic properties associated with the 180-K transition.

DOI: 10.1103/PhysRevB.66.094301 PACS number(s): 63.20.Dj, 71.30.+h, 71.45.Lr

I. INTRODUCTION

A. Transition metal chalcogenides

Transition-metal chalcogenides (TMC) form a group of compounds which can be characterized by an X-M-X structure, where X is a chalcogen and M is a transition metal.[1] The majority of TMC are layered compounds with a hexagonally packed metal layer sandwiched between two chalcogen layers making an X-M-X sandwich. These three-layer sandwiches are weakly bound to each other by weak force, leading to a quasi-two-dimensional behavior in these compounds.

Different arrangements between layers within the sandwich lead to a variety of so-called polytypic modifications. These are indicated by the corresponding prefix to the name of the compound. In particular, the pure octahedral coordination of the metal atom by chalcogen atoms is denoted by $1T$; the pure trigonal prismatic coordinations are denoted by $2H$, $3R$, or $4Hc$; and mixed coordinations are denoted by $4Hb$ or $6R$.[1] The quasi-two-dimensional structure of these materials results in a variety of unique properties. In particular $1T$-TaS_2, which is the subject of this report, was one of the first compounds where a charge-density wave (CDW) was experimentally observed.[1] In this compound the tantalum atoms are octahedrally coordinated by sulphur atoms (see Fig. 1, left panel).

The development of the CDW in $1T$-TaS_2 yields two structural transitions at 350 K and 180 K, with the latter transition demonstrating hysteresis. Both transitions manifest themselves by decrease of the dc conductivity. When the crystal is cooled down the second transition is at $\approx$180 K, whereas when it is warmed up from temperatures below 180 K the transition occurs at $\approx$230 K.

The physics of this compound can be understood in terms of the interaction between the CDW and the crystal lattice. Structural transitions separate the phase diagram into three regions. At temperatures above 350 K there is an incommensurate charge density wave, which becomes nearly commensurate at 350 K. This process is accompanied by the first transition and the formation of a domain structure. Finally at the second transition the CDW becomes completely commensurate. The hysteresis of the second transition

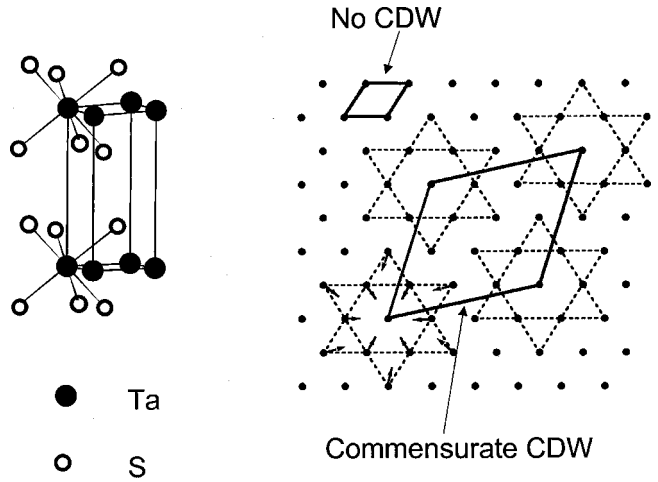

FIG. 1. Structure of $1T$-TaS_2. Left-hand panel shows the unit cell in the normal state (no CDW). The upper part of the right-hand panel shows the arrangement of Ta atoms when no CDW is present. The bottom part of the right-hand panel demonstrates a ''Star-of-David'' cluster formation at a 180-K transition. Small arrows indicate the displacement of Ta atoms when this cluster is formed (Refs. 8 and 9).

($\approx$180 K) is related to the domain structure due to a different orientation of the CDW.

$1T$-TaS_2 has been intensively studied with many different methods. Recently, the interest in this material was revived mainly due to substantial improvements in angle-resolved photoemission spectroscopy (ARPES). In their ARPES studies of this compound Pillo *et al.*[2] observed a rich electronic structure near the Fermi level, with a strong indication of the opening of the gap of $\approx$180 meV below the 180-K transition.

There is a variety of early infrared data on this material.[1,3–7] Since then, progress in infrared spectroscopy equipment has allowed for better sensitivity and resolution, as well as for broader frequency range measurements.

None of the existing publications gives a detailed analysis of the temperature dependance of the frequencies and linewidths of the infrared-active phonons. Nor is there a discussion of the effect of the hysteresis of the 180-K transition on optical data.

We undertook a systematic study of the $1T$-TaS_2 optical reflectance in the frequency range from far infrared to ultraviolet for the temperature range from 30 to 360 K. The effect of the hysteresis on the optical properties of the compound has been also addressed. In this report we discuss our findings in the low-frequency range (below 1000 cm^{-1}) with the main emphasis on the changes in the phonon spectrum of the compound.

B. The charge-density wave and optical phonons in $1T$-TaS_2

Above the 350-K transition, the crystal structure of $1T$-TaS_2 can be described as a CdI_2-type structure belonging to the space group D_{3d}^d, $P\bar{3}2/m1$. The unit cell contains one formula unit (three atoms). As a result, one should expect nine zone-center phonon modes. Group theory predicts the following symmetry in the modes:[7]

$$A_{1g}+E_g+2A_{2u}+2E_u\,.$$

There are two Raman-active modes ($A_{1g}+E_g$) and two infrared-active modes ($A_{2u}+E_u$). The two remaining modes are acoustic phonons. Note that E-type modes are double degenerate.

Below 350 K the CDW becomes nearly commensurate, leading to domains with different orientations of the CDW. Finally at 180 K when the crystal is cooled down, the CDW becomes completely commensurate. This process is accompanied by the formation of the so-called $\sqrt{13}a\times\sqrt{13}a\times 13c$ ''Star-of-David'' cluster. The right panel of Fig. 1 illustrates this process.[8,9] In particular, the Ta atoms in the center of the ''star'' become the corners of a new unit cell. The nearest-neighboring Ta atoms move toward the ''star''-center Ta atoms, and next-nearest-neighboring Ta atoms also move toward it. The displacement of the Ta atoms is accompanied by bulging of the S layers.[10,9] The new unit cell has a C_i^1, $P\bar{1}$ symmetry. It contains 39 atoms and thus leads to a total of 117 modes. Polarized Raman measurements of Uchida and Sugai[7] displayed the selection rules between A_{1g} and E_g modes. It was argued that the symmetry of a single layer (C_{3i}^1, $P3$) can better describe this behavior. Following Uchida and Sugai[7] we expect 117 normal modes,

$$19A_g+20A_u+19E_g+20E_u\,.$$

Thus, there are 38 Raman-active phonon modes ($19A_g+19E_g$) and 40 infrared-active modes ($20A_u+20E_u$). It is clear from this analysis that one should expect a dramatic increase in the number of modes in the low-temperature phase. Some of these new modes are the former Brillouin-zone-boundary modes which become visible because of the increase of the unit cell.

II. EXPERIMENT

The $1T$-TaS_2 single crystals used in this work were grown by chemical vapor transport. This procedure yielded single crystals with a typical size of $10\times10\times0.2$ mm^3. Optical measurements were carried out on the optically smooth surfaces of the as-grown single crystals.

The reflectance was measured in the frequency range of 30–45 000 cm^{-1} (6 meV–5.5 eV) at several temperatures between 30 and 360 K. The sample temperature was maintained by mounting the crystal on the cold finger of a He-flow cryostat. To cover a wide frequency range, we used three optical setups. A Bruker IFS 113V spectrometer was used for the far-infrared and midinfrared regions (50–4500 cm^{-1}; 6–550 meV), a Perkin-Elmer 16U grating spectrometer were used for the near-infrared and visible regions (3800–20 000 cm^{-1}; 0.5–2.5 eV). We observed no temperature dependence of the spectra above 20 000 cm^{-1}. Therefore, in order to extend the data to higher frequencies (20 000–45 000 cm^{-1}; 2.5–5.5 eV) we merged the spectrum at a given temperature with the room-temperature reflectance spectrum obtained from a Zeiss grating spectrometer coupled with a microscope.

In order to analyze the optical properties of the sample we performed a Kramers-Kronig transformation of the reflectance data. For temperatures above 360 K, we used the Drude-Lorentz model fit in the low-frequency part of the spectrum. We calculated the reflectance and used the result for the low-frequency extrapolation. Below the transition, we assumed constant dc conductivity at zero frequency as a low-frequency approximation. For the high-frequency approximation, we used a weak power law followed by free-electronlike behavior.

III. RESULTS AND DISCUSSION

A. Low-frequency optical conductivity and infrared-active phonons

The optical conductivity of $1T$-TaS_2 is shown in Figs. 2 and 3. Notice the strong changes in both the low-frequency optical conductivity as well as in the phonon spectrum. The behavior of the low-frequency conductivity is consistent with a decrease of dc conductivity due to the structural transitions, similar to earlier reported data.[7] At 360 K the phonon modes are strongly screened by free carriers. Only modest traces of the phonon lines are noticeable. The phonon modes

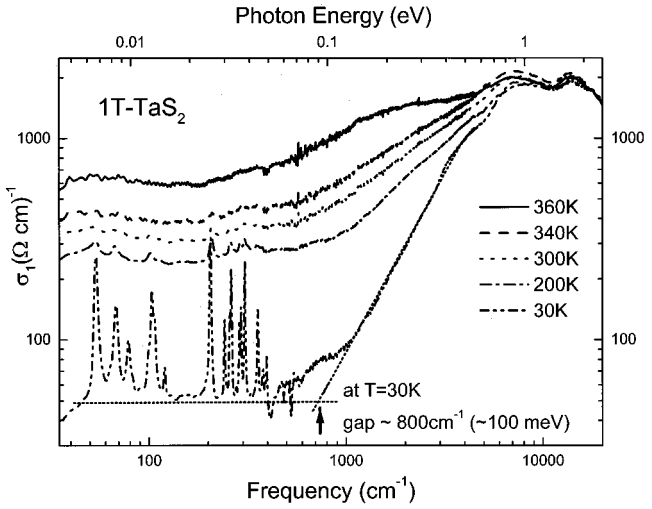

FIG. 2. Temperature dependence of the optical conductivity of $1T$-TaS_2. The gap at 800 cm^{-1} is defined as the onset of the increase of the optical conductivity in the 30-K spectrum. The value of the gap is estimated from the location of the intercept of the background low-frequency optical conductivity and the line representing the increase of the optical conductivity (dashed lines in the 30-K spectrum).

are followed by a pseudo-gap-like increase of the optical conductivity, with direct optical transitions observed at frequencies above 1 eV. Observed changes of charge dynamics in $1T$-TaS_2 will be discussed in a forthcoming publication.

A decrease of the temperature below 360 K leads to a decrease of the low-frequency optical conductivity. A similar decrease is observed in dc conductivity.[2] With this decreased free-electron Drude conductivity the phonon modes become more pronounced. At 200 K one can clearly see at least 11

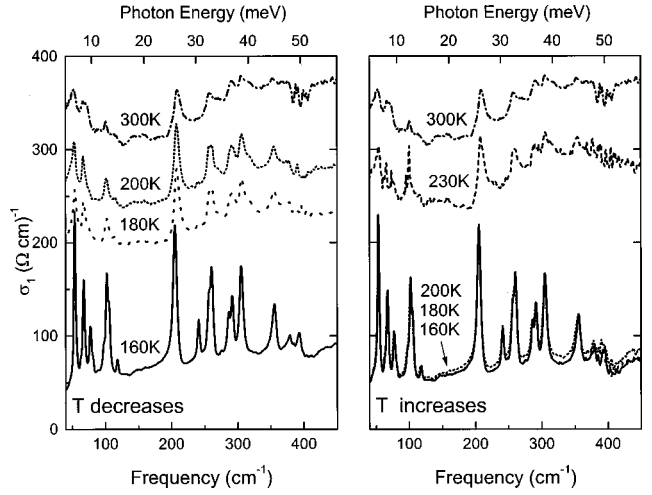

FIG. 3. Hysteresis in the optical conductivity of $1T$-TaS_2. The left-hand panel shows the spectra on the decreasing temperature. The right-hand panel shows spectra on the increasing temperature. Note that spectra at 160 K, 180 K, and 200 K on the right-hand panel are practically indistinguishable. The spectra at the same temperatures but on the decreasing temperature part of the hysteresis are clearly distinguishable.

TABLE I. Slopes of the temperature dependance of the phonon mode frequencies in $1T$-TaS_2.

Phonon frequency (cm^{-1})[a]	Slope (cm^{-1}/K)
54	−0.012
104	−0.013
120[b]	−0.0158
205	0.022
257	−0.011
261	−0.010
287[b]	−0.008
356	−0.013

[a]Only phonons with the frequency change larger than 2 cm^{-1} per 300 K are listed.

[b]This phonon is observed only in the commensurate CDW phase.

phonon modes at 54, 67, 102, 113, 208, 258, 290, 305, 354, 376, and 390 cm^{-1}. This number is much larger than those expected for the two modes in the near-commensurate CDW phase, which could be related to local C_{3i}^1 symmetry already established in this phase.

As the temperature is lowered below ≈180 K, the low-frequency conductivity drops to about one-fifth its value at room temperature; phonon peaks become clearly resolved and the pseudogap develops into a gap. We define this gap as the onset of the increase of the optical conductivity. In Fig. 2, we estimate the value of the gap from the location of the intercept of the background low-frequency optical conductivity at 30 K (50 $\Omega^{-1}\,cm^{-1}$) and the line representing the increase of the optical conductivity (linear dependence on the log-log plot of Fig. 2). From our data we estimate the gap to be of the order of 800 cm^{-1} (100 meV).

At 30 K we clearly see at least 17 phonon modes, at 54, 67, 78, 99, 103, 106, 120, 205, 241, 256, 261, 287, 292, 306, 356, 379, and 395 cm^{-1}. At higher temperatures some of the modes become difficult to separate. For instance only in the low-temperature spectra can we separate the triplet at 99, 103, and 106 cm^{-1}, the doublet at 256 and 261 cm^{-1}; and the doublet at 287 and 292 cm^{-1}. The two modes at 54 and 208 cm^{-1} have the highest intensity. Note that the number of the modes observed in commensurate CDW phase is about half of what was expected from symmetry analysis.

The phonon modes are visibly separated into two groups, Fig. 2. The first group occurs at frequencies below 130 cm^{-1} and the second group at the frequencies above 190 cm^{-1}. Because Ta atoms are about five times heavier than S atoms, we assign the low-frequency group to Ta vibrations and the upper to S vibrations.

We fitted all the observed phonon modes with Lorentzian line shapes in order to obtain their frequency and linewidth. Then we plotted the frequency of the modes versus temperature and fitted these graphs with straight lines. Such an analysis allowed us to estimate the magnitude of the phonon frequency change with the temperature. We considered a change of 2 cm^{-1} over 300 K ($\approx 7\times10^{-3}$ cm^{-1}/K) as the threshold for our analysis. Therefore, only the slopes higher than this threshold are listed in Table I.

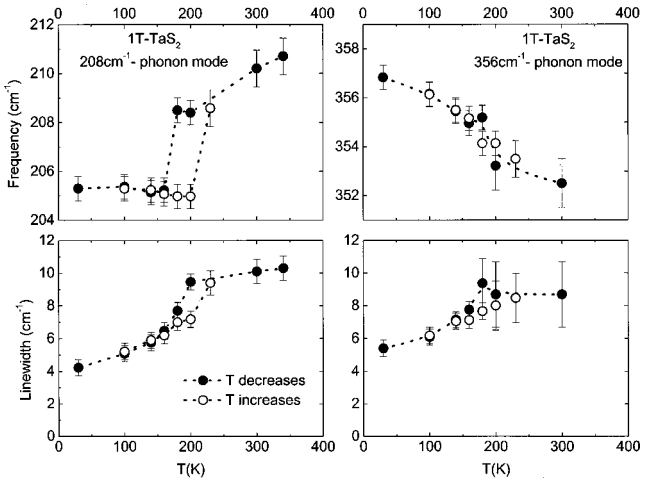

FIG. 4. Hysteresis in the frequency and linewidth of the phonon modes. The left-hand panel shows the frequency (upper part) and linewidth (lower part) of the 208-cm^{-1} phonon mode as a function of temperature. The right-hand panel shows the frequency (upper part) and linewidth (lower part) of the 356-cm^{-1} mode as a function of temperature. The solid circles correspond to the decrease of the temperature and the open circles to its increase. The hysteresis is much stronger for the 208-cm^{-1} mode.

All the modes other than the 208-cm^{-1} mode display the usual decrease of frequency with increase of temperature (negative slope). In contrast, the 208-cm^{-1} mode clearly shows anomalous behavior. As the temperature decreases the frequency of this mode decreases, i.e., this mode softens as shown in Fig. 4. This overall change in frequency with temperature is one of the strongest among the phonon modes in $1T$-TaS_2; see Table I.

The strongest change of frequency of the 208-cm^{-1} mode occurs at the 180-K transition, Fig. 4. We can offer two different scenarios for this effect. Structural changes at the 180-K transition lead to the changes in atomic positions. This in turn means a change in force constants that determine the frequencies of the phonon modes. Such changes can account for the softening of the 208-cm^{-1} mode. One can suggest that this mode is directly coupled to structural changes at the transition. Fazekas and Tosatti[9] proposed that the CDW formation affects not only the Ta layer but the entire S-Ta-S sandwich. It was suggested that sulphur sheets bulge out at the star center. We propose that such a distortion should have an effect on the corresponding phonons.

In the second scenario one can argue that formation of the charge-density wave leads to the disappearance of some parts of the Fermi surface. This in turn leads to the changes in the electronic states interacting with the phonons. The latter causes renormalization of the phonon frequency resulting in the softening of the 208-cm^{-1} mode. A somewhat similar softening of the Raman-active B_{1g} phonon mode[11–21] was observed in $YBa_2Cu_3O_{7-\delta}$ single crystals and was attributed to the strong coupling of the superconducting gap to this phonon.[22,13,23,21,24,25] Both scenario may account for the softening, however, they should be corroborated by theory.

B. The effect of the hysteresis on the spectrum

There is a definite hysteresis in the dc resistivity of $1T$-TaS_2. As a crystal is cooled down, the first transition occurs at 360 K and the second transition occur at approximately 180 K. However when $1T$-TaS_2 is heated from 30 K the same transition occurs at approximately 220 K. Figure 3 demonstrates the effect of hysteresis on optical conductivity. The left panel corresponds to decreasing temperature whereas the right panel represents increasing temperature.

Both the phonon spectrum and the low-frequency conductivity are affected by hysteresis. The effect is especially pronounced for 180-K and 200-K spectra. In particular, the 180-K and 200-K spectra in the left-hand panel of Fig. 3 have low-frequency conductivities of the order of 250 $\Omega^{-1}\,cm^{-1}$, whereas the corresponding spectra in the right-hand panel reveal five times smaller values.

The effect of hysteresis is also clearly seen in the temperature dependence of the frequency and linewidth of the 208-cm^{-1} phonon. The frequency of the mode on the decreasing temperature part of the hysteresis loop is bigger that that measured on the increasing temperature part at the same temperature. This conclusion is also valid for the width of the mode. We checked the same effect for all other modes which could be separated above and below the 180-K transition. We found that the effect is of the order of one wave number which is within experimental error. Corresponding data for the 356-cm^{-1} mode are shown in the right-hand panel of Fig. 4. To our knowledge this is the first observation of such a phonon behavior in $1T$-TaS_2.

IV. CONCLUSIONS

We have presented the results of infrared measurements of $1T$-TaS_2. Both the 350-K and 180-K transitions are accompanied by strong changes in the low-frequency ($\omega < 1000\ cm^{-1}$) conductivity. We observed both additional phonon modes and an anomalous softening of the 208-cm^{-1} phonon at the 180-K transition. This effect shows hysteresis similar to that in dc resistivity. We believe that two competing effects can describe the softening. (i) The first is the lattice effect, when lattice force constants are modified by the structural changes at the transition. Bulging of sulphur layers that accompanies the 180-K transition may account for this effect. (ii) The second is an electronic effect when changes of the electronic states at the Fermi surface due to appearance of the CDW lead to renormalization of the phonon frequency causing the softening of the phonon.

ACKNOWLEDGMENTS

Work at the University of North Florida was supported by Research Corporation Cottrel College Science Award No. CC5290. Work at the University of Florida was supported by NSF Grant Nos. DMR-9705108 and CTS-0082969. The work at the Ecole Polytechnique Fédéral de Lausanne is supported by the Swiss F.N. in part through the NCCR "MaNEP." L.V.G would like to thank E.Ya. Sherman for discussions.

[1] J. A. Wilson and A. D. Yoffe, Adv. Phys. **18**, 193 (1969).
[2] T. Pillo, J. Hayoz, D. Naumović, H. Berger, L. Perfetti, L. Gavioli, A. Taleb-Ibrahimi, L. Schlapbach, and P. Aebi, Phys. Rev. B **64**, 245105 (2001).
[3] A. S. Barker, J. A. Ditzenberger, and F. J. DiSalvo, Phys. Rev. B **12**, 2049 (1975).
[4] G. Lucovsky, W. Y. Liang, and R. M. White, Solid State Commun. **19**, 303 (1976).
[5] D. R. Karecki and B. P. Clayman, Solid State Commun. **19**, 479 (1976).
[6] D. R. Karecki and B. P. Clayman, Phys. Rev. B **19**, 6367 (1979).
[7] S. Uchida and S. Sugai, Physica B & C **105**, 393 (1981).
[8] J. R. Duffey and R. Kirby, Solid State Commun. **20**, 617 (1976).
[9] P. Fazekas and E. Tosatti, Philos. Mag. B **39**, 229 (1979).
[10] J. A. Wilson, F. D. Salvo, and S. Mahajan, Adv. Phys. **24**, 117 (1975).
[11] S. L. Cooper, M. V. Klein, B. G. Pazol, J. P. Rice, and D. M. Ginsberg, Phys. Rev. B **37**, 5920 (1988).
[12] S. Sugai and M. Sato, Phys. Rev. B **40**, 9292 (1989).
[13] B. Friedl, C. Thomsen, and M. Cardona, Phys. Rev. Lett. **65**, 915 (1990).
[14] R. Li, Physica C **175**, 89 (1991).
[15] M. Boekholt, Physica C **185–189**, 1035 (1991).
[16] D. Reznik, Phys. Rev. B **48**, 7624 (1993).
[17] D. H. Leach, Solid State Commun. **88**, 457 (1995).
[18] X. K. Chen, E. Altendorf, J. C. Irwin, R. Liang, and W. N. Hardy, Phys. Rev. B **48**, 10 530 (1993).
[19] E. Altendorf, Phys. Rev. B **47**, 8140 (1993).
[20] M. Kakihana, M. Osada, M. Käll, L. Börjesson, H. Mazaki, H. Yasuoka, M. Yashima, and M. Yoshimura, Phys. Rev. B **53**, 11 796 (1996).
[21] T. Devereaux, A. Virosztek, A. Zawadowski, M. Opel, P. Muller, C. Hoffman, R. Philip, R. Nemetschek, R. Hackl, and H. Berger, Solid State Commun. **108**, 407 (1998).
[22] E. I. Rashba and E. Y. Sherman, JETP Lett. **47**, 482 (1988).
[23] T. Devereaux, A. Virosztek, and A. Zawadowski, Phys. Rev. B **51**, 505 (1995).
[24] E. Sherman, R. Li, and R. Feile, Solid State Commun. **94**, 851 (1995).
[25] E. Sherman, R. Li, and R. Feile, Phys. Rev. B **52**, R15 757 (1995).